

Hydrogen Species and Anionic Vacancies on Heteropolycompounds Catalytic Hydrogen Reservoirs

L. Jalowiecki-Duhamel,^{*,1} A. Monnier,^{*} and Y. Barbaux[†]

^{*}Laboratoire de Catalyse Hétérogène et Homogène, U.R.A., C.N.R.S. N° 402, Université des Sciences et Technologies de Lille, 59655 Villeneuve d'Ascq Cedex, France; and [†]Université d'Artois, SP 18, rue J. Souvraz, 62307 Lens Cedex, France

Received July 8, 1997; revised November 24, 1997; accepted January 29, 1998

A dynamic method of titration is used to provide evidence for reactive hydrogen (H^*) present in different heteropolycompounds (HPC). This method of titration involves hydrogenation of 2-methylbuta-1,3-diene (isoprene) under helium flow in the absence of gaseous hydrogen and permits to reveal and titrate reactive hydrogen species (H^*) that a solid is able to store. The heteropolycompounds are catalytic hydrogen reservoirs with marked diffusion properties for hydrogen species (H^* , OH^-). The hydrogen reservoir capacity depends on the pretreatment temperature under H_2 , which has been shown to correspond to the creation of anionic vacancies in the solid by the loss of H_2O . In the conditions in which the incorporation of hydrogen in the solids occurs, *in-situ* X-ray diffraction analysis under H_2 show shifts, depending on the treatment temperature and corresponding to a lattice expansion attributed mainly to the insertion of hydrogen species of hydridic nature in the anionic vacancies. © 1998 Academic Press

INTRODUCTION

This last 20 years the key role of hydrogen has become widely evident for energy storage, in metallurgy as well as in heterogeneous catalysis (1). The nature of hydrogen is under controversy. It is usually admitted that hydrogen adsorption on a metal or other surfaces able to adsorb hydrogen is dissociative. The problem is if the rupture is heterolytic or homolytic. Therefore, four different species can be created and transported: the radical H^\cdot , the bonded species H^- , or the charged species H^+ , or H^- .

The literature relating the use of heteropolyoxometalates (HPC) for isomerization reactions, etherification reactions, or methanol conversion to hydrocarbons, indicates systematically that *a priori* reduction of the HPC under H_2 , or either the presence of H_2 in the reactant mixture is a prerequisite condition for the reaction to be observed or to be markedly enhanced (2–8). Some other studies show that the reduction under H_2 of the HPC implies the loss of “constitution”

water (3, 9, 10). The formation of “constitution” water after reduction of the HPC corresponds to the loss of lattice oxygen and leads to the creation of anionic vacancies if the structure is maintained.

Besides, numerous studies mention the ability of HPC to store, after reduction, some hydrogen species which are not evacuated as water. Baba *et al.* have determined 2.32 moles per mole of polyanion of hydrogen inserted in $Ag_3PW_{12}O_{40}/SiO_2$ reduced under 40 kPa at 488 K for 1 h (6). By Proton NMR, X-ray diffraction, and IR the same authors have shown that the chemisorption of H_2 is “reversible” and that the hydrogen species generated in the HPC by reduction under H_2 present a higher mobility than the protons initially present in the HPC. Yoshida *et al.* have determined that, under a programmed thermoreduction, the $Ag_3PMo_{12}O_{40}$ and $Cu_{1.5}PMo_{12}O_{40}$ compounds present hydrogen adsorption peaks with higher intensities compared to $Ag_3PW_{12}O_{40}$ and $Cu_{1.5}PW_{12}O_{40}$ (11). Finally, it has been shown that the mixed compounds Mo–W adsorb the highest quantity of hydrogen (12). In agreement with these results, the reduction rate under H_2 to 1 e^- /U.K. and the reoxydation rate by O_2 at 623 K are the highest for PW_6Mo_6 , compared to PMo_{12} , PW_{12} , $PMo_{11}V$, and $PMo_{10}V_2$ (12). Moreover, the presence of Ag, Cu, or Pd decrease the temperature at which the HPC is able to store hydrogen species (9). Therefore, $H_3PMo_{12}O_{40}$ and $H_3PMo_6W_6O_{40}$ supported on Pd/C are able to adsorb hydrogen at an ambient temperature.

Baba *et al.* have observed by solid NMR on $Ag_3PW_{12}O_{40}$ reduced under H_2 , three peaks related to hydrogen (13). The first peak at 4.1 ppm corresponds to the water formed during the reduction, the second peak at 6.4 ppm is attributed to a hydrogen species of acid nature because the corresponding peak disappears after treatment under pyridine atmosphere at 303 K for 30 min. The last peak at 9.3 ppm starts to decrease only when the second peak at 6.4 ppm has disappeared. The authors attributed these hydrogen species to another type of proton. In fact, in the literature the hydrogen species are proposed to be H^+ species.

¹ To whom correspondence should be addressed. E-mail: Louise.Duhamel@univ-lille1.fr.

TABLE 1

Composition of the Different HPC and Method of Introduction of the Counteranions

HPC composition/Mo	Counteranion introduction
$(\text{NH}_4)_{2.5}\text{Cs}_{1.6}\text{P}_{1.7}\text{Mo}_{11}\text{V}_{1.1}\text{O}_{40}$	$\text{CsCO}_3 + \text{NH}_4\text{Cl}$
$(\text{NH}_4)_{3.5}\text{Ce}_{0.16}\text{P}_{1.3}\text{Mo}_{11}\text{V}_{1.2}\text{O}_{40}$	$\text{CeNO}_3 + \text{NH}_4\text{Cl}$
$(\text{NH}_4)_{3.5}\text{Ce}_{0.09}\text{P}_{1.2}\text{Mo}_{11}\text{V}_{1.0}\text{O}_{40}$	$\text{CeNO}_3 + \text{NH}_4\text{Cl}$
$(\text{NH}_4)_{2.0}\text{Ce}_{0.16}\text{Cs}_{1.65}\text{P}_{1.3}\text{Mo}_{11}\text{V}_{1.2}\text{O}_{40}$	$\text{CeNO}_3 + \text{CsCO}_3 + \text{NH}_4\text{Cl}$
$\text{P}_{1.4}\text{Mo}_{11}\text{V}_{1.2}\text{O}_{40}$	—
$\text{Ce}_{0.19}\text{P}_{1.1}\text{Mo}_{11}\text{V}_{1.0}\text{O}_{40}$	$\text{Ba}(\text{OH})_2; \text{Ce}_3(\text{SO}_4)_2$
$\text{Cu}_{0.19}\text{P}_{1.1}\text{Mo}_{11}\text{V}_{1.0}\text{O}_{40}$	$\text{Ba}(\text{OH})_2; \text{Cu}(\text{SO}_4)$
$\text{Cs}_{1.8}\text{P}_{1.1}\text{Mo}_{11}\text{V}_{1.1}\text{O}_{40}$	CsCO_3

We propose in this study to analyze the behavior and interactions between anionic vacancies and hydrogen species (H^* and/or OH^-) in heteropolycompounds.

EXPERIMENTAL

The heteropolyacid ($\text{H}_4\text{PMo}_{11}\text{VO}_{40}$) was prepared first by a method presented in Ref. (14) slightly modified. The different heteropolycompounds (HPC) were obtained by adding the stoichiometric quantity of different salts as presented in Table 1 to an aqueous solution of $\text{H}_4\text{PMo}_{11}\text{VO}_{40}$. The resulting suspension was evaporated to dryness at 393 K, 10 h. The loading was measured before and after catalytic test by microanalysis by the Centre d'Analyses du CNRS of Vernaison. One must remark, that the ammonium loading uncertainty is high; therefore the values presented in Table 1 are those attended and those measured are of the same order. After the catalytic test, NH_4^+ is eliminated.

The dynamic method which allows us to provide evidence for and to determine the concentration of reactive and extractable hydrogen H^* species has been previously reported (15, 16). The pretreatment and catalytic experiments were carried out at atmospheric pressure in an all-glass grease-free flow apparatus. The catalyst was treated *in-situ* under purified hydrogen flow at various temperatures T_T between 473 and 623 K for 12 h. After each treatment step under H_2 , the solid (300 mg) was cooled to 423 K. Isoprene was then introduced at constant pressure (6 to 8 Torr—1 Torr = 133.3 Nm^{-2}) in an isothermal reactor (423 K) and then the mixture H_2 + isoprene is replaced by a mixture of He + isoprene. The total elimination of gaseous hydrogen was followed by the use of a catharometer, after 4 min the concentration of molecular hydrogen in the gas phase was lower than 0.1%.

Isoprene (2-methylbuta-1,3-diene), purum grade from Fluka, was used after purification by distillation under vacuum. Hydrogen and helium (N-55 grade) came from Air Liquide. The reaction products were analyzed by gas chro-

matography using a capillary column (squalane, 0.2 mm ID, 100-m long) operating at 313 K and a flame ionisation detector.

The structures of the solids were analyzed in a Siemens D5000 diffractometer equipped with an Anton Paar HTK 10 chamber and connected to a gas introduction and purification line. A position-sensitive detector was used; the flow conditions and the rate of temperature increase were similar to those adopted in thermogravimetry. Apart from the $K\alpha_2$ contribution eliminated by computer postprocessing, the patterns obtained were not subjected to further treatments. Owing to the use of a platinum holder, they show platinum diffraction peaks, the evolution of which with T_T was taken into account in determining the exact position of the peaks of the solids analysed.

The thermogravimetric experiments were carried out under purified hydrogen in a Sartorius balance. The solids were treated under a hydrogen flow (5 liter/h) and the temperature was increased at a rate of 1.7 $\text{K} \cdot \text{min}^{-1}$.

RESULTS

I. Anionic Vacancies

The thermoreductions under H_2 have been performed, and the results obtained on $(\text{NH}_4)_{2.5}\text{Cs}_{1.6}\text{P}_{1.7}\text{Mo}_{11}\text{V}_{1.1}\text{O}_{40}$, $(\text{NH}_4)_{3.5}\text{Ce}_{0.16}\text{P}_{1.3}\text{Mo}_{11}\text{V}_{1.2}\text{O}_{40}$, and $\text{Ce}_{0.19}\text{P}_{1.1}\text{Mo}_{11}\text{V}_{1.0}\text{O}_{40}$ are presented in Fig. 1. In agreement with the literature (17, 18), up to 473 K, the weight loss observed corresponds to the loss of crystallisation water. For temperatures higher than 473 K, a continuous loss of water and ammonium is observed for $(\text{NH}_4)_{2.5}\text{Cs}_{1.6}\text{P}_{1.7}\text{Mo}_{11}\text{V}_{1.1}\text{O}_{40}$ up to 753 K, and for $(\text{NH}_4)_{3.5}\text{Ce}_{0.16}\text{P}_{1.3}\text{Mo}_{11}\text{V}_{1.2}\text{O}_{40}$ up to 728 K. The global weight loss after 473 K is 17.7% for $(\text{NH}_4)_{3.5}\text{Ce}_{0.16}\text{P}_{1.3}\text{Mo}_{11}\text{V}_{1.2}\text{O}_{40}$ and 15.7% for $(\text{NH}_4)_{2.5}\text{Cs}_{1.6}\text{P}_{1.7}\text{Mo}_{11}\text{V}_{1.1}\text{O}_{40}$. On $\text{Ce}_{0.19}\text{P}_{1.1}\text{Mo}_{11}\text{V}_{1.0}\text{O}_{40}$, the weight

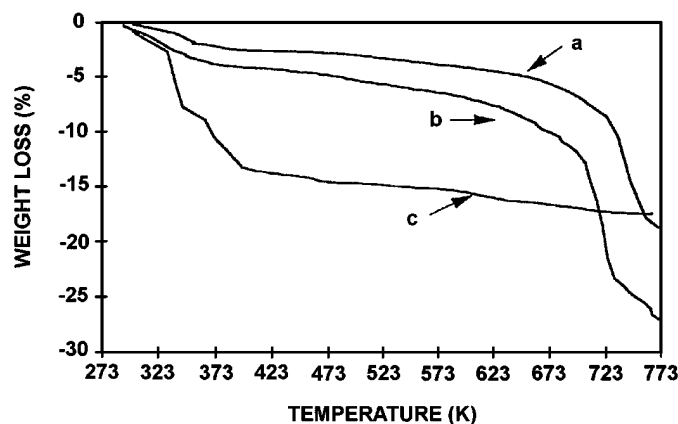


FIG. 1. Thermal treatment under H_2 of (a) $(\text{NH}_4)_{2.5}\text{Cs}_{1.6}\text{P}_{1.7}\text{Mo}_{11}\text{V}_{1.1}\text{O}_{40}$, (b) $(\text{NH}_4)_{3.5}\text{Ce}_{0.16}\text{P}_{1.3}\text{Mo}_{11}\text{V}_{1.2}\text{O}_{40}$, and (c) $\text{Ce}_{0.19}\text{P}_{1.1}\text{Mo}_{11}\text{V}_{1.0}\text{O}_{40}$, followed by thermogravimetry.

loss observed for temperatures higher than 473 K is about 4 wt%, which is much lower than the weight loss obtained on the two other HPC for which one must consider the elimination of NH_4^+ . Knowing that Ce present as a counter-cation in $\text{Ce}_{0.19}\text{P}_{1.1}\text{Mo}_{11}\text{V}_{1.0}\text{O}_{40}$ has been introduced by a method involving a barium salt, it is probable that there are only residual sulfates as impurities. Concerning the other two HPC, the counter-cations have been introduced respectively as cerium nitrate + ammonium chloride and cesium carbonate + ammonium chloride. The carbonates are eliminated as CO_2 when adding the counter-cation. The nitrates and chlorides remain as impurities. Admitting that these impurities are totally eliminated and taking into account the complete elimination of ammonium in this range of temperatures, the real weight loss attributable to water can be respectively 7.3 and 9.7% for $(\text{NH}_4)_{3.5}\text{Ce}_{0.16}\text{P}_{1.3}\text{Mo}_{11}\text{V}_{1.2}\text{O}_{40}$ and $(\text{NH}_4)_{2.5}\text{Cs}_{1.6}\text{P}_{1.7}\text{Mo}_{11}\text{V}_{1.1}\text{O}_{40}$.

The “constitution” water results in the association of acidity protons with oxygen atoms of the polyanion, and this phenomenon is reversible in the presence of water (19–21). The loss of “constitution” water can be resumed by the equation reported for phosphomolybdic acid (22),



with \square = anionic vacancy.

According to the literature, ammonium reduces partially the catalyst during its evacuation (23, 24). Therefore, the higher weight loss observed for $(\text{NH}_4)_{3.5}\text{Ce}_{0.16}\text{P}_{1.3}\text{Mo}_{11}\text{V}_{1.2}\text{O}_{40}$ and $(\text{NH}_4)_{2.5}\text{Cs}_{1.6}\text{P}_{1.7}\text{Mo}_{11}\text{V}_{1.1}\text{O}_{40}$, compared to $\text{Ce}_{0.19}\text{P}_{1.1}\text{Mo}_{11}\text{V}_{1.0}\text{O}_{40}$, can be due to the supplementary reducing power of NH_4^+ which accelerates *in-situ* the reduction of the HPC. The quantity of H_2O formed and lost for the compounds containing ammonium in their precursor state is therefore increased, which permits us to enhance the number of anionic vacancies created.

II. Hydrogen H^*

Titration. In a previous study, we reported that after treatment under H_2 , $\text{Cs}_{1.6}\text{H}_{2.4}\text{P}_{1.7}\text{Mo}_{11}\text{V}_{1.1}\text{O}_{40}$ contains anionic vacancies produced by the elimination of H_2O (OH groups) and also some reactive hydrogen species able to hydrogenate alkadienes in the absence of gaseous hydrogen (25, 26). These species are denoted H^* as we are not considering their exact charge. At 423 K, under a helium + isoprene flow, alkadiene hydrogenation occurs on H_2 -treated HPC as presented in Fig. 2 for $(\text{NH}_4)_{2.5}\text{Cs}_{1.6}\text{P}_{1.7}\text{Mo}_{11}\text{V}_{1.1}\text{O}_{40}$. It is important to note that the hydrogenation activity obtained on the untreated solid is null. As a function of time on-stream, the isoprene conversion or hydrogenation activity (HYD) is measured. The ratio ($\text{HYD}_{\text{rel}} = A_{\text{Ht}}/A_{\text{H0}}$ (where A_{H0} and A_{Ht} are the initial hydrogenation and the hydrogenation activity at time t) can be plotted versus time; this relative hydrogenation activity at

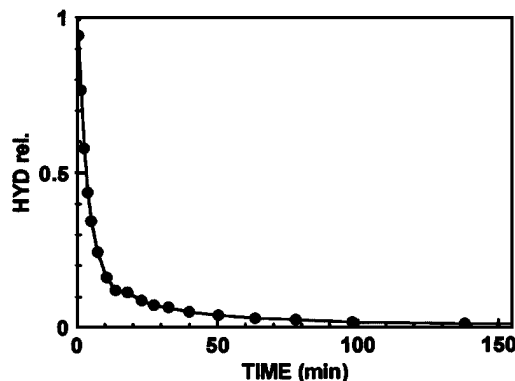


FIG. 2. Relative hydrogenation activity at 423 K under helium + isoprene flow versus time on $(\text{NH}_4)_{2.5}\text{Cs}_{1.6}\text{P}_{1.7}\text{Mo}_{11}\text{V}_{1.1}\text{O}_{40}$ treated in H_2 at 623 K.

423 K under helium + alkadiene feed decreases with time. For each solid a similar curve is obtained and by integrating this curve the extractable reactive hydrogen content of the solid can be determined if the product distribution is taken into account (2H^* for monohydrogenation and 4H^* for dihydrogenation).

The extractable H^* content found on the HPC previously treated under H_2 at 623 K are reported in Table 2. One can remark that the HPC containing ammonium in the precursor state such as $(\text{NH}_4)_{2.5}\text{Cs}_{1.6}\text{P}_{1.7}\text{Mo}_{11}\text{V}_{1.1}\text{O}_{40}$ are the largest hydrogen reservoirs. The highest value found in the range of temperatures studied is of $1.3 \times 10^{-3} \text{ mol} \cdot \text{g}^{-1}$ which corresponds to 2.7 moles per mole of HPC, in good agreement with some values presented in the literature (9). As a matter of fact, Baba *et al.* have reported that $\text{Ag}_3\text{PW}_{12}\text{O}_{40}/\text{SiO}_2$ is able to store 2.32 moles of hydrogen per mole of HPC (13). Moreover, it appears that the H^* concentration depends on the treatment temperature under H_2 (Table 3). For the two HPC presented, almost no H^* is found for T_{T} lower than 523 K, and the H^* content increases with the treatment temperature up to 623 K.

Diffusion. In addition, between t and t_f (time at which the hydrogenation activity is found to be 0), the percentage

TABLE 2

Hydrogen H^* Content of the Different HPC Treated under H_2 at 623 K

HPC Composition/Mo	$\text{H}^* 10^3 \text{ mol} \cdot \text{g}^{-1}$	$\text{H}^* \text{ mole/mole}_{\text{HPC}}$
$(\text{NH}_4)_{2.5}\text{Cs}_{1.6}\text{P}_{1.7}\text{Mo}_{11}\text{V}_{1.1}\text{O}_{40}$	1.3	2.7
$(\text{NH}_4)_{3.5}\text{Ce}_{0.16}\text{P}_{1.3}\text{Mo}_{11}\text{V}_{1.2}\text{O}_{40}$	1.3	2.6
$(\text{NH}_4)_{3.5}\text{Ce}_{0.09}\text{P}_{1.2}\text{Mo}_{11}\text{V}_{1.0}\text{O}_{40}$	1.1	2.15
$(\text{NH}_4)_{2.0}\text{Ce}_{0.16}\text{Cs}_{1.65}\text{P}_{1.3}\text{Mo}_{11}\text{V}_{1.2}\text{O}_{40}$	0.33	0.7
$\text{P}_{1.4}\text{Mo}_{11}\text{V}_{1.2}\text{O}_{40}$	0.001	0.002
$\text{Ce}_{0.19}\text{P}_{1.1}\text{Mo}_{11}\text{V}_{1.0}\text{O}_{40}$	0.018	0.04
$\text{Cu}_{0.19}\text{P}_{1.1}\text{Mo}_{11}\text{V}_{1.0}\text{O}_{40}$	0.034	0.07
$\text{Cs}_{1.8}\text{P}_{1.1}\text{Mo}_{11}\text{V}_{1.1}\text{O}_{40}$	0.31	0.64

TABLE 3

Hydrogen H^* Content as a Function of the Treatment Temperature under H_2

HPC	Treatment temperature under H_2 $H^* 10^3 \text{ mol} \cdot \text{g}^{-1}$		
	523 K	593 K	623 K
$(\text{NH}_4)_{2.5}\text{Cs}_{1.6}\text{P}_{1.7}\text{Mo}_{11}\text{V}_{1.1}\text{O}_{40}$	0.04	1.2	1.3
$(\text{NH}_4)_{3.5}\text{Ce}_{0.16}\text{P}_{1.3}\text{Mo}_{11}\text{V}_{1.2}\text{O}_{40}$	0	1.4	1.3

of reactive hydrogen still present in the solid can be estimated. As an example, HYD_{rel} versus H^*_{rel} concentration data is presented in Fig. 3 for $(\text{NH}_4)_{2.5}\text{Cs}_{1.6}\text{P}_{1.7}\text{Mo}_{11}\text{V}_{1.1}\text{O}_{40}$ and $(\text{NH}_4)_{2.0}\text{Ce}_{0.16}\text{Cs}_{1.65}\text{P}_{1.3}\text{Mo}_{11}\text{V}_{1.2}\text{O}_{40}$ treated in H_2 at 623 K. The curves obtained on the different solids clearly show that there is no proportionality between the relative hydrogenation rate consuming H^* and the H^* content of the solid. The kinetics of H^* consumption by the alkadiene is a complex phenomenon which has been widely studied (15, 27); in particular, a fast diffusion process of the H^* species within the solid must be considered.

For the HPC which are large hydrogen reservoirs ($[H^*] \geq 1.1 \times 10^{-3} \text{ mol} \cdot \text{g}^{-1}$), the variation of isoprene hydrogenation activity as a function of time under helium (Fig. 2) corresponds to a specific hydrogenated products distribution presented in Fig. 4 for $(\text{NH}_4)_{2.5}\text{Cs}_{1.6}\text{P}_{1.7}\text{Mo}_{11}\text{V}_{1.1}\text{O}_{40}$. Whereas for the HPC which store low quantities of hydrogen ($[H^*] \leq 0.33 \times 10^{-3} \text{ mol} \cdot \text{g}^{-1}$) no isopentane is observed and the different products obtained decrease regularly with time on stream, these compounds present low hydrogenating activities. Isoprene hydrogenation activity takes into account all the hydrogenated products, which are isopentane (dihydrogenated), 2-methylbut-1-ene (2MB1), 3-methylbut-1-ene (3MB1), and 2-methylbut-2-

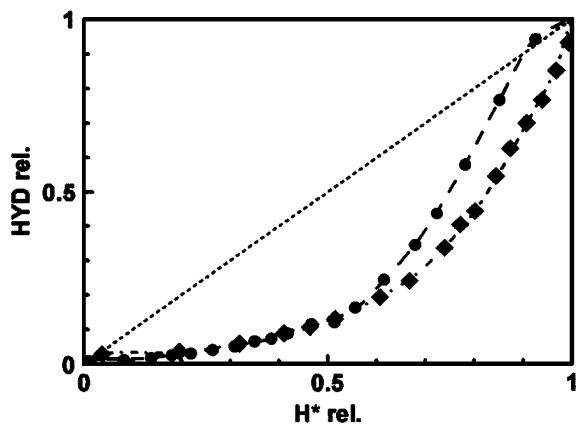


FIG. 3. Relative hydrogenation activity at 423 K under helium + isoprene flow versus hydrogen H^* species concentration of (●) $(\text{NH}_4)_{2.5}\text{Cs}_{1.6}\text{P}_{1.7}\text{Mo}_{11}\text{V}_{1.1}\text{O}_{40}$ and (◆) $(\text{NH}_4)_{2.0}\text{Ce}_{0.16}\text{Cs}_{1.65}\text{P}_{1.3}\text{Mo}_{11}\text{V}_{1.2}\text{O}_{40}$ treated in H_2 at 623 K.

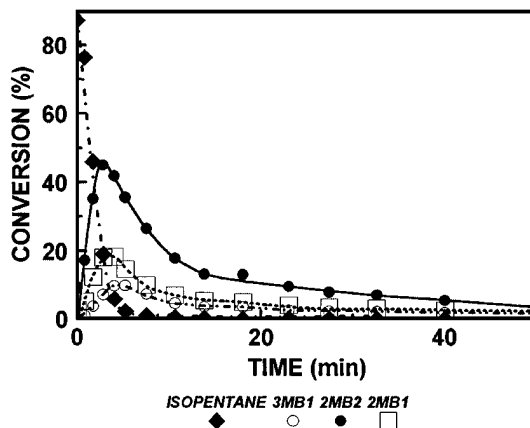


FIG. 4. Isoprene hydrogenated products distribution at 423 K as a function of time under helium on $(\text{NH}_4)_{2.5}\text{Cs}_{1.6}\text{P}_{1.7}\text{Mo}_{11}\text{V}_{1.1}\text{O}_{40}$ treated in H_2 at 623 K.

ene (2MB2) (monohydrogenated). The direct analysis of the curves obtained in Fig. 4 reveals different areas, as has been already observed and defined previously on different copper-based oxides (16). When molecular hydrogen disappears completely from the gas phase a sharp decrease of activity is observed. At the same time the production of isopentane also decreases drastically, whereas the production of monoenes formed changes. Maxima are reached successively by 2-methylbut-2-ene and the two methylbut-1-enes. Moreover, 3-methylbut-1-ene starts to increase when 2-methylbut-2-ene disappears. No simple correlation is found between the time of isopentane disappearance or the appearance of maxima of formation of the various products and either the H^* content.

It can be recalled that similar behaviour is also observed on sulfides ($\text{MoS}_2/\text{Al}_2\text{O}_3$) for which a good correlation has been obtained between the selectivity and the site structure (28). Similar variations of isoprene product distribution under helium + isoprene flow as a function of time have also been obtained with various H^* species concentrations. It has been shown that a small number of active sites are sufficient to produce a large quantity of isopentane when the hydrogen reservoir is large enough. However, even though the amount of H^* hydrogen species in the solid is high, the formation of isopentane is null when the corresponding active sites do not exist.

III. In Situ XRD

Under H_2 . The *in-situ* X-ray diffraction has been performed on two different HPC which crystallise in the cubic phase, $(\text{NH}_4)_{2.5}\text{Cs}_{1.6}\text{P}_{1.7}\text{Mo}_{11}\text{V}_{1.1}\text{O}_{40}$ and $(\text{NH}_4)_{3.5}\text{Ce}_{0.16}\text{P}_{1.3}\text{Mo}_{11}\text{V}_{1.2}\text{O}_{40}$. The evolution of the XRD spectra of the HPC when treated under H_2 as a function of the temperature is presented in Figs. 5 and 6. No drastic crystallographic modification is evidenced. However, a careful examination

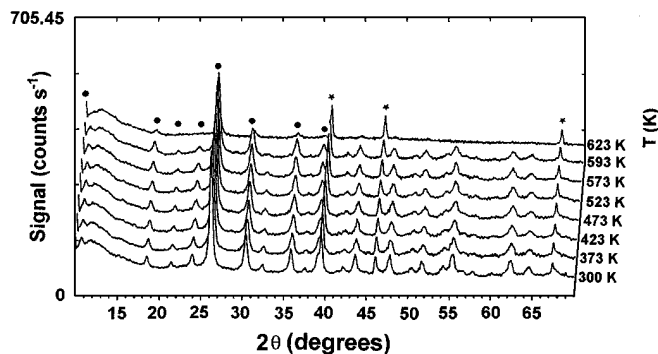


FIG. 5. XRD patterns during *in-situ* treatment under H_2 of the cubic $(NH_4)_{2.5}Cs_{1.6}P_{1.7}Mo_{11}V_{1.1}O_{40}$ compound (●), platinum (★).

shows that, each diffraction line is shifted towards lower angles for treatment temperatures higher than 473 K (Fig. 7). In order to specify the conditions in which the expanded phase has been formed during the reduction treatment, the peak position has been plotted as a function of T_T for the most intense lines. Reported in Figs. 8 and 9 is the difference $\Delta 2(\theta)$ between the initial peak position (300 K) and its position at T_T , corrected from the thermal expansion factor (the $\Delta(2\theta)$ value is given within an accuracy of $\pm 0.02^\circ$). Several hypothesis can be evoked to account for the variation of the cell parameter, the reduction of some metallic cations and/or the incorporation of hydrogen. The interaction of hydrogen with a series of mixed oxides CeM_x ($M = Cu, Ni$; $0 < x < 5$) has been studied in the 300–1073 K temperature range. XPS, EPR, *in-situ* XRD, and thermogravimetric techniques have been used to characterize the processes occurring during the hydrogen treatment and the amount of hydrogen occluded in the solids when treated at different temperatures under H_2 (29, 30).

The evolution of the XRD spectra of the H_2 treated at 623 K $Cs_{1.8}P_{1.1}Mo_{11}V_{1.1}O_{40}$ compound as a function of time is presented in Table 4. This compound has a much lower

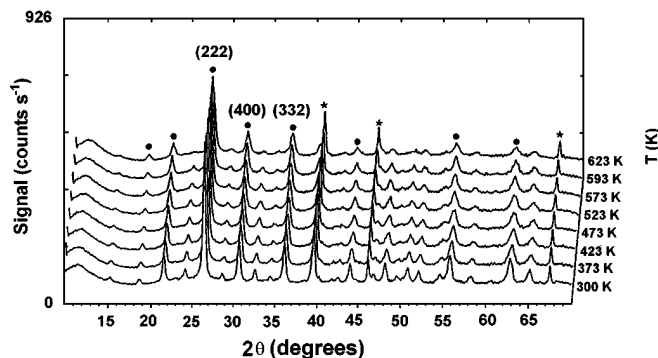


FIG. 6. XRD patterns during *in-situ* treatment under H_2 of the cubic $(NH_4)_{3.5}Ce_{0.16}P_{1.3}Mo_{11}V_{1.2}O_{40}$ compound (●), platinum (★).

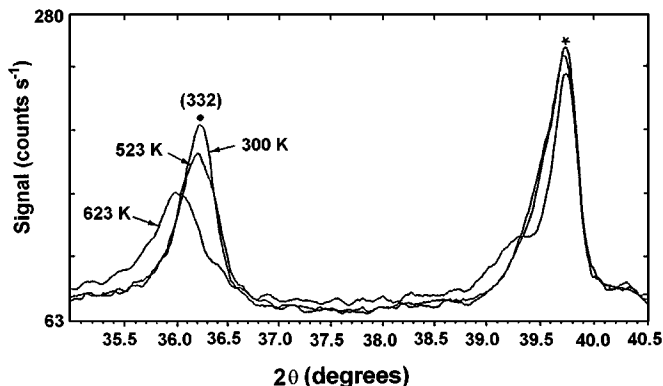


FIG. 7. Zoom of the 332 line ($\approx 36.2^\circ$) of Fig. 6: $(NH_4)_{3.5}Ce_{0.16}P_{1.3}Mo_{11}V_{1.2}O_{40}$ compound (●); platinum (★).

ability to store hydrogen, but the results are interesting because this compound does not contain ammonium in its precursor phase; therefore it is important to see that the diffraction shift still exists, so it is not due to a direct effect of the presence of ammonium.

Under nitrogen. In order to get more information about the eventual role of ammonium, and in particular, if the presence of ammonium in the precursor phase of the solid can lead to the insertion in the solid of hydrogen species, similar experiments have been performed under nitrogen. In Table 5 are presented the results obtained on two different compounds, $Cs_{1.8}P_{1.1}Mo_{11}V_{1.1}O_{40}$ and $(NH_4)_{2.5}Cs_{1.6}P_{1.7}Mo_{11}V_{1.1}O_{40}$. The last one contains ammonium in its precursor phase in total substitution of the residual protons. The measure is performed under N_2 at 623 K as a function of time, i.e. elimination of NH_4^+ . The variation in $\Delta 2(\theta)$ is presented for the most intense peaks. Each diffraction line is shifted toward the lower angles for $(NH_4)_{2.5}Cs_{1.6}P_{1.7}Mo_{11}V_{1.1}O_{40}$, whereas no shift is observed for $Cs_{1.8}P_{1.1}Mo_{11}V_{1.1}O_{40}$.

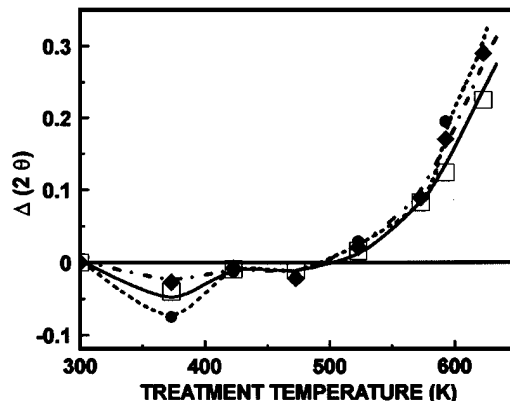


FIG. 8. Shift of the diffraction peaks in $(NH_4)_{2.5}Cs_{1.6}P_{1.7}Mo_{11}V_{1.1}O_{40}$ during *in-situ* treatment under H_2 : (□) 222; (◆) 400, (●) 332.

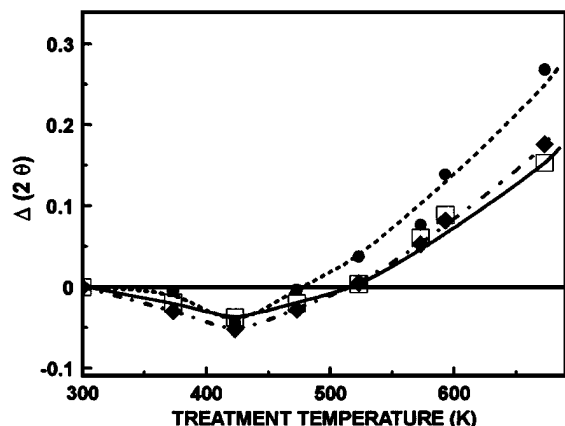


FIG. 9. Shift of the diffraction peaks in $(\text{NH}_4)_{3.5}\text{Ce}_{0.16}\text{P}_{1.3}\text{Mo}_{11}\text{V}_{1.2}\text{O}_{40}$ during *in-situ* treatment under H_2 : (\square) 222; (\blacklozenge) 400; (\bullet) 332.

DISCUSSION

Evidence is provided for the existence of particular reactive hydrogen species of the solid. Even if the hydrogen uptake by the HPC has already been reported in the literature, it has been attributed to the formation of H^+ species (9, 13). Nevertheless, in the present study, the H^* species are able to hydrogenate alkadienes at 423 K without the presence of H_2 when the solid has been previously treated under H_2 ; otherwise no H^* species is found. Hence the hydroxyl groups (OH) always present on the solid cannot justify the results obtained. Moreover, it appears that the H^* concentration depends on the treatment temperature under H_2 (Table 3), almost no H^* is found for T_T lower than 523 K, and the H^* content increases with the treatment temperature up to 623 K.

For treatment temperatures higher than 523 K, anionic vacancies are created in the catalyst produced by the elimination of water (OH groups), as controlled by thermogravimetry under H_2 (Fig. 1). Several studies show that the reduction under H_2 of the HPC implies the loss of lattice oxygen and leads to the formation of anionic vacancies if the structure is maintained (3, 9, 10). The Keggin structure really seems to be conserved for these treatment temperatures as it has been shown that the reduced HPC are more

TABLE 4

$\Delta(2\theta)$ Measured on $\text{Cs}_{1.8}\text{P}_{1.1}\text{Mo}_{11}\text{V}_{1.1}\text{O}_{40}$ when Treated under H_2 at 623 K as a Function of Time

Time under H_2 at 623 K	$\text{Cs}_{1.8}\text{P}_{1.1}\text{Mo}_{11}\text{V}_{1.1}\text{O}_{40}$		
	$2\theta \sim 26^\circ 2$	$2\theta \sim 30^\circ 4$	$2\theta \sim 35^\circ 7$
1 h 30	0.005	0.05	0.04
2 h	0.06	0.10	0.16

Note. The $\Delta(2\theta)$ value is given within an accuracy of $\pm 0.02^\circ$.

TABLE 5

$\Delta(2\theta)$ Measured on $(\text{NH}_4)_{2.5}\text{Cs}_{1.6}\text{P}_{1.7}\text{Mo}_{11}\text{V}_{1.1}\text{O}_{40}$ and $\text{Cs}_{1.8}\text{P}_{1.1}\text{Mo}_{11}\text{V}_{1.1}\text{O}_{40}$ when Treated under Nitrogen at 623 K as a Function of time

HPC	2θ	$\Delta(2\theta)$ as a function of time under N_2 at 623 K			
		0.5 h	5.5 h	10.5 h	15.5 h
$(\text{NH}_4)_{2.5}\text{Cs}_{1.6}\text{P}_{1.7}\text{Mo}_{11}\text{V}_{1.1}\text{O}_{40}$	$\sim 26.3^\circ$	0.14	0.18	0.18	0.19
	$\sim 30.3^\circ$	0.11	0.20	0.21	0.21
	$\sim 35.7^\circ$	0.16	0.19	0.24	0.28
$\text{Cs}_{1.8}\text{P}_{1.1}\text{Mo}_{11}\text{V}_{1.1}\text{O}_{40}$	$\sim 26.3^\circ$	0.00	0.00	0.02	0.01
	$\sim 30.3^\circ$	0.01	0.00	0.02	0.02
	$\sim 36.7^\circ$	-0.01	0.01	0.00	0.01

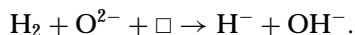
stable thermally than the nonreduced HPC. As a matter of fact, no decomposition of the heteropolyacid (HPA) has been reported before 773 K on $\text{H}_3\text{PMo}_{12}\text{O}_{40}$ reduced to $2 e^-$ (31), and before 693 K on $\text{H}_3\text{PMo}_{12}\text{O}_{40}$ reduced to $6.4 e^-$ (13). Hodnett *et al.* have estimated the temperature of decomposition of $\text{H}_3\text{PMo}_{12}\text{O}_{40}$ at about 773 K (32). In the same way, it has been shown, by mass spectrometry, that the nonreduced HPC could also loose some "constitution" water at temperatures lower than those of their decomposition, while the results of X-ray diffraction indicated that the primary Keggin structure is conserved in these conditions (33). Therefore, for the HPC this loss of water is obtained between 593 and 623 K (17, 18, 34).

As a function of the treatment under H_2 , before the decomposition of the HPC, the number of anionic vacancies increases. Therefore, there exists a correlation between the creation of anionic vacancies with the H^* species storage in the solid. The anionic vacancies are able to store reactive hydrogen species, which quantity increases with the treatment temperature up to 623 K. A great analogy exists between these results and those obtained in our laboratory on copper-based oxides (16) and on Mo-based sulfides (35, 36).

Taking into account previous studies which have shown that the hydrogenation mechanism can be described in terms of a nucleophilic attack of the diene which leads to the formation of anionic intermediates (37), all the results are consistent with a heterolytic splitting of H_2 . One half of the hydrogen reservoir (H^*) consists of hydride ions, H^- , and the other half is protons, H^+ , provided by the hydroxyl groups (OH^-). Considering the relative size of H^- and O^{2-} (1.54, and 1.32 Å, respectively), the lattice expansion observed in the reduction step under H_2 corresponds to the substitution of an O^{2-} species by an H^- species, even if a contribution of some reduced cations has also to be considered.

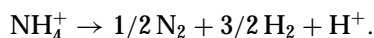
Therefore, the insertion in the solid of a particular hydrogen species created by heterolytic splitting of H_2 (H^- located in an anionic vacancy and H^+ forming with an

O^{2-} species an OH^- group) can be summarized as follows:



The insertion of H^+ species in the HPC has been much more often proposed in the literature than the insertion in the solid of H^- species; anyway, in the case of a heterolytic rupture the two species (H^- , H^+) can exist, but due to its high reactivity (as for example with O_2), the H^- species is not easy to detect.

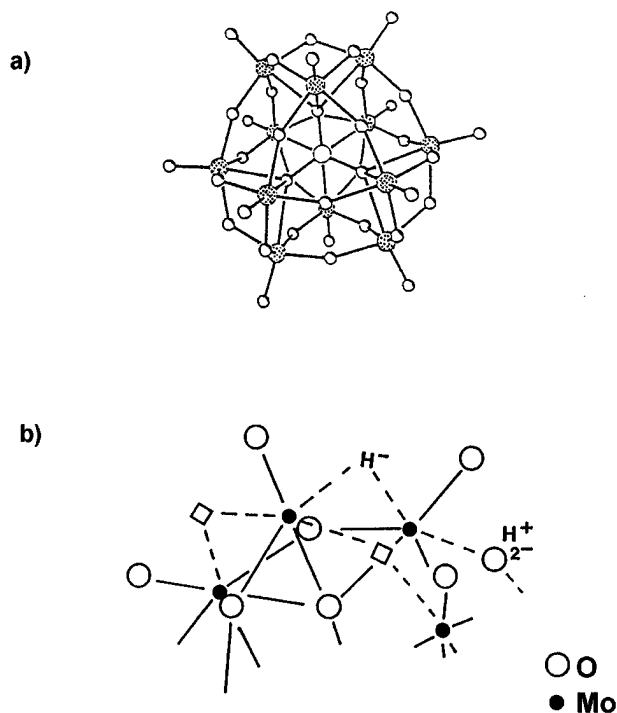
For solids containing NH_4^+ in the precursor phase, some hydrogen species can be inserted in the solid when treating in temperature under nitrogen. During its elimination, NH_4^+ is probably transformed to H_2 and N_2 :



The 40 oxygen atoms of the polyanion are not all equivalent; therefore the anionic vacancies created can be also different. After the loss of crystallisation water, the protons can be bound to the terminal oxygen atoms (2), but it has been also proposed that the bridged oxygen atoms between P and Mo correspond to P–O–Mo bonds which are long and weak (38–40). Based on molecular orbital calculations on 12-heteropolymolybdates, some other authors proposed that the bridged oxygen atoms Mo–O–Mo have the higher probability of being associated to acidity protons and leave the polyanion as “constitution” water (9, 41). Therefore, the anionic vacancies created can be terminal and/or bridged and shared by several cations. One must remark that the bridged anionic vacancies have the possibility to be in higher concentration, because for 12 oxygen atoms bound to one metallic atoms, there are 28 oxygen atoms shared by two metallic atoms. Scheme 1 presents a possible modeling, based on an initial Keggin structure. The position of the anionic vacancies is arbitrary; they can be terminal and/or bridged between cations of the same nature or not (Mo–O–Mo, Mo–O–V, ...), the presence of the counteranion increases even the number of possibilities. One must recall that the dehydration of the HPC is still under controversy.

Moreover, the hydrogen reservoir properties, as presented previously, largely involve diffusion processes of reactive hydrogen species H^* . The change of gas phase to a helium + isoprene mixture involves a decrease of the activity, which reaches 0 in a time dependent on the reservoir capacity. This variation of activity is accompanied by a particular variation of the products distribution (Fig. 4).

The presence of anionic vacancies has been seen as necessary to obtain catalytic activity. Evidence has been provided of their role in lattice diffusion phenomena (42, 43). By analogy with homogeneous catalysis, Siegel has defined three different coordinatively unsaturated sites (CUS) with



SCHEME 1. (a) Conventional atomic representation of the Keggin unit $PMo_{12}O_{40}^{3-}$. (b) Generated site under H_2 on a HPC with an initial Keggin-type structure.

1, 2, or 3 unsaturations on the cation (1M , 2M , or 3M) in chromium and cobalt oxides. The 3M and 2M sites have been respectively associated with alkadiene hydrogenation and isomerization reactions (44, 45). The concept has been validated and widely used by Tanaka and co-workers (46–49). Thus if the hydrogenation reaction is associated with 3M sites, it appears reasonable to correlate isopentane coming from a double hydrogenation of isoprene with a 3M – $^3M'$ ensemble, where each cation is 3 CUS (16). In fact, the xM – $^yM'$ ensemble composed of two cations (with x and y the unsaturation degrees of each cation) is correlated with the combination of the corresponding reactions (hydrogenation, isomerization) occurring on each cation.

In the present study, for the HPC able to contain more than $1.1 \text{ mol} \cdot \text{g}^{-1}$ of hydrogen H^* , the 3M – $^3M'$ ensembles exist because isopentane is obtained among the products. The 3M – $^3M'$ ensembles are stable under a flow of H_2 + isoprene at 423 K, because the reactive hydrogen species H^* consumed by the hydrogenation reaction can be regenerated by heterolytic rupture of molecular hydrogen (16). However, it is highly probable that these elementary ensemble sites with some high degree of unsaturation are unstable in the absence of gaseous hydrogen; therefore the substitution of H_2 by He leads to a sharp decrease of isopentane which rapidly reaches zero.

The result obtained is a blocking of the sites associated with the production of isopentane (^3M - $^3\text{M}'$) simultaneously with the creation of ^3M - $^2\text{M}'$ sites correlated with 2-methylbut-2-ene formation resulting from a hydrogenation + isomerisation reaction. The concentration of 2-methylbut-2-ene attains a maximum corresponding to a maxima of ^3M - $^2\text{M}'$ sites, which become ^3M - $^1\text{M}'$ sites before a final transformation to ^3M - $^0\text{M}'$ ensembles. When the ^3M site disappears, the hydrogenation activity cannot be observed anymore. This phenomenon, also observed on intermetallic systems (50), has been detailed in copper-based mixed oxide studies (16) and related to OH group migration. During the consumption of the H^* species the unsaturation degree of the site varies and decreases. As a matter of fact, if the hydrogen H^* species are for one-half H^- species, they are also for the other half H^+ species (coming from OH groups). The H^* species are "pumped" to the surface by the hydrocarbon and consumed by hydrogenation reaction, and this supposes the migration of H^- and H^+ species. It appears that it is the hydroxyl group which diffuses and, once the H^+ species is consumed, the O^{2-} species remains in the anionic vacancy and decreases the unsaturation degree of the site (16).

CONCLUSION

The heteropolycompounds are shown to be hydrogen reservoirs with marked diffusion properties for the hydrogen species. The hydrogen storage depends on the treatment temperature under H_2 , i.e. to the creation of anionic vacancies, as the structure is maintained in the range of the temperatures studied. Therefore, it is proposed that the insertion of hydrogen in the solid is obtained by heterolytic splitting of H_2 (H^- , H^+) in agreement with the results obtained by *in-situ* X-ray diffraction analysis under H_2 . As a matter of fact X-ray diffraction analysis under H_2 show shifts depending on the treatment temperature and corresponding to a lattice expansion attributed to the insertion of hydrogen species of hydridic nature in the anionic vacancies.

ACKNOWLEDGMENT

We gratefully acknowledge Elf-Atochem for financial support.

REFERENCES

1. Paal, Z., and Menon, P. G. (Eds.), "Hydrogen Effects in Catalysis," p. 1. Dekker, New York, 1988.
2. Ono, Y., and Baba, T., in "8th Int. Cong. Catal., 1984," Vol. 5, p. 405.
3. Baba, T., Watanabe, H., and Ono, Y., *J. Phys. Chem.* **87**, 2406 (1983).
4. Ono, Y., Taguchi-Gerile, M., Suzuki, S., and Baba, T., *Stud. Surf. Sci. Catal.* **20**, 167 (1985).
5. Ono, Y., and Baba, T., *Hom. Heter. Catal.*, in "Proceedings, 5th International Symp. Rel., 1986," p. 273.
6. Baba, T., Nomura, M., Ono, Y., and Kansaki, Y., *J. Chem. Soc. Farad. Trans.* **88**, 71 (1992).
7. Suzuki, S., Kogai, K., and Ono, Y., *Chem. Lett.* **5**, 699 (1984).
8. Na, K., Okuhara, T., and Misono, M., *J. Chem. Soc. Chem. Comm.* **18**, 1422 (1993).
9. Katamura, K., Nakamura, T., Sakata, K., Misono, M., and Yoneda, Y., *Chem. Lett.* **1**, 89 (1981).
10. Eguchi, K., Toyozawa, Y., Yamazoe, N., and Seiyama, T., *J. Catal.* **83**, 32 (1983).
11. Yoshida, S., Niiyama, H., and Echigoya, E., *J. Phys. Chem.* **86**, 3150 (1982).
12. Misono, M., Igarashi, H., Katamura, K., Okuhara, T., and Mizuno, N., *Stud. Surf. Sci. Catal.* **77**, 105 (1993).
13. Baba, T., Nomura, M., Ohno, Y., Hiroyama, Y., and Ono, Y., *Stud. Surf. Sci. Catal.* **77**, 281 (1985).
14. Courtin, P., *Rev. Chim. Min.* **8**, 75 (1971).
15. Jalowiecki, L., Daage, M., Bonnelle, J. P., and Tchen, A., *Appl. Catal.* **16**, 1 (1985).
16. Sene, A., Jalowiecki-Duhamel, L., Wrobel, G., and Bonnelle, J. P., *J. Catal.* **144**, 544 (1993).
17. Tsigdinos, *Ind. Eng. Chem. Prod. Res. Dev.* **13**, 267 (1974).
18. Feumi-Jantou, C., Ph.D. thesis, Paris VI, France, 1989.
19. Marchal, C., Ph.D. thesis, Paris VI, France, 1991.
20. Misono, M., Komaya, T., Sekiguchi, H., and Yoneda, Y., *Chem. Lett.* **1**, 53 (1982).
21. Moffat, J. B., in "4th Int. Symp. Scientific Basis for the Preparation of Heterogeneous Catalysts, Louvain la Neuve, 1986."
22. Kazansky, L. P., Potapova, I. V., and Spitsyn, V. I., in "Proceedings, 3rd International Conference on the Chemistry and Uses of Molybdenum, 1979," p. 67.
23. Yamaguchi, Y., Yamamatsu, S., Kawakami, K., Suzuki, Y., and Aoshima, A., "Comm. Asahi Chem. Co. Autumn Meeting of Japan Chem. Soc., 1991."
24. Albonnetti, S., Cavani, F., Trifiro, F., Gazzano, M., Koutyrev, M., Aissi, F. C., Aboukais, A., and Guelton, M., *J. Catal.* **146**, 491 (1994).
25. Jalowiecki-Duhamel, L., Monnier, A., Barbaux, Y., and Hecquet, G., *Catal Today* **32**, 237 (1996).
26. Jalowiecki-Duhamel, L., Lamonier, C., Monnier, A., Barbaux, Y., and Wrobel, G., in "Proceedings, 11th World Hydrogen Energy Conference, Stuttgart, Germany, 1996" (T. N. Veziroglu, C.-J. Winter, J. P. Baselt, and G. Kreysa, Eds.), Vol. 2, p. 1253.
27. Jalowiecki, L., Wrobel, G., Daage, M., and Bonnelle, J. P., *J. Catal.* **107**, 375 (1987).
28. Duhamel-Jalowiecki, L., Sene, A., Wrobel, G., and Grimblot, J., *Int. J. Hydrogen Energy* **18**, 925 (1985).
29. Wrobel, G., Sohler, M. P., D'Huysser, A., and Bonnelle, J. P., *Appl. Catal. A: General* **101**, 73, (1993).
30. Wrobel, G., Lamonier, C., Bennani, A., D'Huysser, A., and Aboukais, A., *J. Chem. Soc. Farad. Trans.* **92**, 2001 (1996).
31. Chuvaev, V. F., Popov, K. F., and Spitsyn, V. I., *Dokl. Akad. Nauk SSSR* **243**, 973 (1978).
32. Hodnett, B. K., and Moffat, J. B., *J. Catal.* **91**, 93 (1985).
33. Hodnett, B. K., and Moffat, J. B., *J. Catal.* **88**, 253 (1988).
34. Misono, M., *Mater. Chem. Phys.* **17**, 103 (1987).
35. Jalowiecki, L., Aboulaz, A., Kasztelan, S., Grimblot, J., and Bonnelle, J. P., *J. Catal.* **120**, 108 (1989).
36. Jalowiecki, L., Grimblot, J., and Bonnelle, J. P., *J. Catal.* **126**, 101 (1990).
37. Daage, M., and Bonnelle, J. P., *Appl. Catal.* **16**, 355 (1985).
38. Bruckman, K., Tatibouet, J. M., Che, M., Serwicka, E., and Haber, J., *J. Catal.* **139**, 455 (1993).
39. King, R. B., *Inorganic Chem.* **30**, 4437 (1991).

40. Pope, M. T., and Muller, A., *Angew. Chem. Int. Ed. Engl.* **30**, 34 (1991).
41. Eguchi, K., Seiyama, T., Yamazoe, N., Katsuki, S., and Taketa, H., *J. Catal.* **111**, 336 (1988).
42. Murch, G. E., and Nowick, A. S. (Eds.), "Diffusion in Crystalline Solids," Chap. 3. Academic Press, Orlando, FL, 1984.
43. Sanchez, M. G., and Gazquez, J. L., *J. Catal.* **104**, 120 (1987).
44. Siegel, S., *J. Catal.* **30**, 139 (1973).
45. Siegel, S., Outlaw, J., and Garti, N., *J. Catal.* **52**, 102 (1978).
46. Takeuchi, A., Tanaka, K. I., and Miyahara, K., *Chem. Lett.* 171, and 411 (1974).
47. Tanaka, K. I., and Okuhara, T., *Catal. Rev. Sci. Eng.* **15**, 24 (1977).
48. Tanaka, K. I., *Adv. Catal.* **33**, 99 (1985).
49. Tanaka, K. I., and Okuhara, T., in "Proceedings, 3rd International Conference on the Chemistry and Uses of Molybdenum" (H. F. Barry and P. C. H. Mitchell, Eds.), p. 170. Climax Molybdenum Company, Ann Arbor, MI, 1980.
50. Pinabiau, M., Ph.D. thesis, Lille, France, 1987.